

The Reversible Magnesiumation of Pb

Kalani Periyapperuma, Tuan T. Tran, M.I. Purcell, M.N. Obrovac*

Department of Chemistry, Dalhousie University, Halifax, NS, Canada, B3H 4R2

*corresponding author: mnobrovac@dal.ca

Abstract

Sputtered Pb films have been found to reversibly alloy electrochemically with magnesium in Grignard based electrolytes. The voltage curve shows a single plateau at about 125 mV vs. Mg, corresponding to the formation of Mg_2Pb , as confirmed by ex-situ X-ray diffraction. Pb was found to be the highest energy density Mg alloy yet reported, with the lowest voltage and highest volumetric capacity of any Mg alloy

Introduction

Rechargeable magnesium batteries have been long considered as a promising technology for energy storage and conversion. The low cost, low electrochemical potential and high volumetric and specific capacity of Mg makes it attractive as a negative electrode for secondary batteries.¹⁻³ However, a passivation layer is formed at the Mg electrode surface in common polar aprotic electrolyte solvents blocks both Mg ions and electron transport.³ Reversible stripping and plating at the magnesium electrode has only been demonstrated in highly volatile ethereal-based solvents, such as tetrahydrofuran (THF)³ or 1,2-dimethoxyethane (DME).^{4,5} It would be desirable to enable the use of non-volatile electrolytes with low flammability for the development of practical Mg batteries.

Alloys have been suggested for use as the negative electrode instead of Mg metal.⁶ It has further suggested that the passivation layer on Mg metal electrodes might be avoided if Mg

1
2
3
4 alloys are used as the negative electrode.^{7,8} Arthur et. al demonstrated C-rate cycling of
5
6 electrodeposited Bi, Sb and Bi-Sb alloys.⁷ Bi forms Mg_3Bi_2 upon full magnesianation,
7
8 corresponding to 384 mAh/g or 1897 Ah/L, with an average voltage of about 250 mV vs Mg. Sb
9
10 forms Mg_3Sb_2 upon full magnesianation, corresponding to 660 mAh/g or 2040 Ah/L, with an
11
12 average voltage of about 325 mV vs Mg. When cycled versus a 1.2 V Mo_6S_8 cathode, the
13
14 theoretical energy density of Bi and Sb are about 1800 Wh/L. 100 cycles with low capacity fade
15
16 at C-rate was demonstrated for Bi electrodes. When Sb was added to make Bi-Sb alloys, both
17
18 rate and fade progressively worsened. This was thought to be due to the increased Mg-Sb bond
19
20 strength compared to Mg-Bi. Arthur et al. also showed reversible magnesianation from a Bi
21
22 electrode in a $Mg(N(SO_2CF_3)_2)_2$ (hereafter denoted as $Mg(TFSI)_2$) in acetonitrile. Recently, Shao
23
24 et al. have shown reversible magnesianation of nano-structured Bi for hundreds of cycles in
25
26 diglyme-based electrolytes.⁸ Furthermore, the nanostructure allowed high rates of up to 5C to be
27
28 sustained.
29
30
31
32
33
34
35

36 Here we consider Pb as another potential anode material for rechargeable magnesium ion
37
38 batteries. Lead is inexpensive, making it attractive for use in commercial batteries. Although lead
39
40 is toxic, lead acid batteries are successfully used in the majority of the > 1 billion automobiles on
41
42 the planet. This made possible by the implementation recovery/recycling programs.⁹ Given this
43
44 enormous precedent, we consider Pb-containing electrodes a viable and inexpensive possibility
45
46 for use in cells, when effective recycling programs are in place.
47
48
49
50
51
52

53 **Experimental**

54
55 Pb was sputtered deposited onto 13 mm stainless steel (SS) foil discs using a modified
56
57 Corona Vacuum Coater V-3T deposition system. A base pressure of 7.6×10^{-7} Torr with a 3.1
58
59
60
61
62
63
64
65

1
2
3
4 mTorr argon pressure and a 35 W target power were used during the deposition process. The SS
5
6 discs were weighed before and after sputtering using a Satorius SE-2 microbalance ($\pm 0.1 \mu\text{g}$
7
8 resolution), in order to determine the mass of the sputtered Pb film. The average thickness of the
9
10 sputtered Pb film was $0.24 \mu\text{m}$. After sputtering, the discs were transferred immediately in to an
11
12 argon filled glovebox to minimize the oxidation of Pb. Composite electrodes were made from Pb
13
14 powder (~ 325 mesh, 99%, Sigma Aldrich), poly(vinylidene fluoride) (PVDF, HSV 900,
15
16 KYNAR) and Super P carbon black (SP, EraChem, Europe) in a 80/10/10 mass ratio and cast
17
18 from NMP (anhydrous 99.5%, Sigma Aldrich) onto SS foil, followed by air drying at 120°C for
19
20 2 hours. The average electrode loading was 2.4 mg/cm^2 .
21
22
23

24
25
26 Conflat cells, as described in reference,¹⁰ were constructed using sputtered disc or
27
28 composite lead electrodes and Mg foil (99.95%, 0.25 mm thick, Gallium Source, LLC, Scotts
29
30 Valley, CA) counter/reference electrodes. All cells were constructed in an argon filled glovebox.
31
32 Two layers of Celgard 2300 separator were used in each cell with a layer of polyethylene blown
33
34 microfiber separator (BMF, 3M Company) in between. The BMF provides a compliant layer,
35
36 which improves stack pressure distribution. An electrolyte solution of 0.5 M ethylmagnesium
37
38 chloride (EtMgCl, Sigma Aldrich) with or without 0.25 M AlCl_3 (anhydrous, 99.985%, Alfa
39
40 Aesar) in tetrahydrofuran (THF, $< 2 \text{ ppm H}_2\text{O}$, 99.9%, inhibitor free, Sigma Aldrich) was used in
41
42 cells. Cells were cycled at C/40, C/50 or C/100 rate between 5 mV and 250 mV vs. Mg at $60 \pm$
43
44 0.1°C . Here C-rate was calculated based on the formation of Mg_2Pb at full magnesiation. All
45
46 cells were cycled under thermostatically controlled conditions ($\pm 0.1^\circ\text{C}$) using a Maccor Series
47
48 4000 Automated Test System.
49
50
51
52
53

54
55 Ex-situ x-ray diffraction pattern (XRD) measurements were made by disassembling cells
56
57 at different states of charge, rinsing the working electrode in THF and drying under vacuum to
58
59
60
61
62
63
64
65

1
2
3
4 evaporate the solvent prior sealing in an air sensitive X-ray sample holder under an argon
5
6 atmosphere. XRD measurements were collected using a Rigaku Ultima IV diffractometer
7
8 equipped with a Cu K α radiation source, and a scintillation detector with a graphite diffracted
9
10 beam monochromator.
11

12 13 14 15 16 **Results and Discussion** 17

18
19 Figure 1 shows the voltage curve of a Pb/Mg two electrode Conflat cell cycled at C/50
20
21 rate at 60°C. At this initial cycling rate, the cell continues to discharge well beyond the
22
23 theoretical capacity of Pb (517 mAh/g). This is suggestive that catalytic reactions are occurring
24
25 at the Pb electrode surface with the electrolyte that consume Mg ions and do not allow the
26
27 magnesiation of Pb to proceed. This effect has been observed previously on Sn surfaces in Li-
28
29 ion¹¹ and Na-ion cells¹² and on Pb surfaces in Na-ion cells.¹³ In Li-ion cells, such catalytic
30
31 reactions can be avoided with the use of proper additives.¹⁴ However, in Grignard reagents no
32
33 analogously functioning additives are known. Another method to avoid catalytic electrolyte on
34
35 alloy surfaces is to apply a high initial current pulse to the cell prior to discharge.¹¹⁻¹³ This is
36
37 believed to cause a thin layer of the catalytic metal surface to alloy with Li or Na, rendering it
38
39 non-catalytic.
40
41
42
43
44

45
46 In order to magnesiate the surface of Pb and inhibit reactivity with the electrolyte, cells
47
48 were initially held at a constant voltage of 5 mV for 3 minutes and then the cell was allowed to
49
50 rest for few minutes at open circuit voltage prior to constant current cycling. As shown in Figure
51
52 2, after the initial voltage hold, reversible cycling commenced. So little charge was passed
53
54 through the cell during the initial voltage hold that it appears in the voltage curve as a vertical
55
56 spike at the beginning of discharge. The voltage curve consists of a single plateau, indicative of a
57
58
59
60
61
62
63
64
65

1
2
3
4 simple 2-phase reaction. The plateau has a low average voltage of about 125 mV, which is the
5
6 lowest voltage yet reported for a magnesium alloy. Voltage polarization during cycling is also
7
8 low for an alloy (~ 25 mV), indicating good kinetics. The mean voltage between both plateaus of
9
10 about 138 mV agrees well with previous estimates of the Gibbs free energy of formation at 198
11
12 K for Mg₂Pb of -46.6 kJ/mol (or 121 mV vs. Mg).¹⁵ The reversible capacity for magnesianation is
13
14 about 450 mAh/g. This is slightly less than the theoretical capacity for the formation of Mg₂Pb
15
16 (517 mAh/g). We attribute this difference to weighing error in our thin sputtered film. The
17
18 formation of Mg₂Pb corresponds to a rather large volumetric capacity of about 2300 Ah/L, which
19
20 is three times greater than that of graphite in a lithium ion cell and is the highest volumetric
21
22 capacity reported for a magnesium alloy.
23
24
25
26
27

28
29 Figure 3 shows the cycling performance of the sputtered Pb film electrode. The
30
31 coulombic efficiency is poor, as the voltage curve slips to the right during cycling. The discharge
32
33 capacity exceeds the charge capacity by about 14% each cycle. Electrode slippage is associated
34
35 with electrolyte decomposition reactions that consume the active ion at the working electrode.¹⁶
36
37 For Li-ion battery materials, high precision coulometry is needed to detect slippage, as the
38
39 slippage is usually within the error of conventional battery chargers. Here the slippage is so large
40
41 that a conventional battery charger can easily detect it. After only 8 cycles the voltage curve slips
42
43 in an amount that exceeds the reversible capacity of the electrode. Such a high rate of slippage
44
45 indicates that Pb is poorly passivated in this electrolyte, which is surprising considering the
46
47 stability of THF.¹⁷ However even though Mg is irreversibly consumed by the side reactions,
48
49 there is a continuous supply of Mg from the counter/reference electrode; therefore little
50
51 demagnesianation capacity loss occurs during cycling.
52
53
54
55
56
57
58
59
60
61
62
63
64
65

1
2
3
4 To understand the structural changes that occur during cycling, electrochemical cells
5
6 were disassembled at different states for ex-situ XRD studies of the sputtered Pb electrodes.
7
8 Figure 4(c) shows the XRD pattern of a pristine sputtered Pb electrode. The pattern is that of
9
10 phase pure Pb. Figure 4(b) shows an ex-situ XRD pattern of a sputtered Pb electrode after being
11
12 discharged to 5 mV. The majority phase in the XRD pattern is Mg₂Pb, however a small amount
13
14 of Pb remains unreacted in the electrode. Two peaks at 21.0° and 23.4° in the XRD pattern are
15
16 suspected to be from electrolyte residue left on the Pb electrode surface. Figure 4(a) shows an
17
18 ex-situ XRD pattern of a sputtered Pb electrode after it has been discharged to 5 mV, and then
19
20 charged to 0.25 V. The XRD peaks are now completely due to Pb, excepting some electrolyte
21
22 residue peaks at 21.0° and 23.4°, as before. The peaks at fully charged state agree well with the
23
24 XRD pattern of pristine Pb, as shown in Figure 4(c). Therefore the magnesianation of Pb follows
25
26 the equilibrium phase diagram according to:
27
28
29
30
31



32
33
34
35
36 Figure 5 shows the voltage curve of a Pb composite coating vs. Mg. It is similar to the sputtered
37
38 coating shown in Figure 2, excepting that a low voltage and sloping plateau is present and grows
39
40 during cycling. This plateau was also present in the voltage curve of some sputtered films. We do
41
42 not know the origin of this plateau, although it resembles that which occurs near the full
43
44 lithiation of Sn.¹⁸ Near full lithiation, Sn forms disordered Li_xSn clusters, with sloping voltage
45
46 plateaus.¹⁹ Perhaps a similar mechanism occurs here. Such phases are difficult to detect by XRD
47
48 and we could find no evidence any new phases formed at this plateau by ex-situ XRD.
49
50
51

52
53 Figure 6 shows the cycling performance of the Pb composite coating vs. Mg cell shown
54
55 in Figure 5. The irreversible capacity of this cell is ~114 mAh/g and is considerably higher than
56
57 that of the cell with sputtered deposited Pb electrode. The reversible capacity is only about 275
58
59
60
61
62
63
64
65

1
2
3
4 mAh/g, which is much less than that of the sputtered electrode. Pb particles may have become
5
6 disconnected during cycling or Mg may not be able to access the core of the particles, which
7
8 have a much larger diameter than the sputtered film. Like the sputtered film, the electrode
9
10 slippage is high and coulombic efficiency is low. Improved electrolyte stability is required to
11
12 improve the cycling performance of these electrodes.
13
14
15
16
17
18

19 **Conclusion**

20
21 Magnesium was reversibly inserted in sputtered and composite Pb electrodes, forming
22
23 Mg_2Pb in a 2-phase reaction with a theoretical capacity of 2300 Ah/L, which is the highest
24
25 volumetric capacity reported for an Mg alloy. In addition the Pb vs. Mg voltage curve has the
26
27 lowest voltage (~125 mV) of any Mg alloy. Therefore, Pb was found to be the highest energy
28
29 density alloy material yet reported in Mg batteries. However, extremely poor coulombic
30
31 efficiencies were observed that are indicative of electrolyte decomposition reactions at the Pb
32
33 surface during cycling. Improved electrolyte stability is required to improve the performance of
34
35 these electrodes.
36
37
38
39
40
41
42

43 **Acknowledgments**

44
45 The authors acknowledge funding from NSERC auspices of the Discovery Grants
46
47 program. We also acknowledge the support of the Canada Foundation for Innovation and the
48
49 Atlantic Innovation Fund.
50
51
52
53
54
55
56
57
58
59
60
61
62
63
64
65

References

1. D. Aurbach, Y. Gofer, Z. Lu, A. Schechter, O. Chusid, H. Gizbar, Y. Cohen, V. Ashkenazi, M. Moshkovich, R. Turgeman, *Journal of Power Sources*, **97-98** , 28 (2001).
2. D. Aurbach, Z. Lu, A. Schechter, Y. Gofer, H. Gizbar, R. Turgeman, Y. Cohen, M. Moshkovich, E. Levi, *Nature*, **407** (6805) , 724 (2000).
3. H.D. Yoo, I. Shterenberg, Y. Gofer, G. Gershinsky, N. Pour, D. Aurbach, *Energy & Environmental Science*, **6** (8) , 2265 (2013).
4. R.E. Doe, R. Han, J. Hwang, A.J. Gmitter, I. Shterenberg, H.D. Yoo, N. Pour, D. Aurbach, *Chemical Communications (Cambridge, England)*, **50** (2) , 243 (2014).
5. R. Mohtadi, M. Matsui, T.S. Arthur, S.-J. Hwang, *Angewandte Chemie (International Ed. in English)*, **51** (39) , 9780 (2012).
6. T.T. Tran, M.N. Obrovac, *Journal of The Electrochemical Society*, **158** (12) , A1411 (2011).
7. T.S. Arthur, N. Singh, M. Matsui, *Electrochemistry Communications*, **16** (1) , 103 (2012).
8. Y. Shao, M. Gu, X. Li, Z. Nie, P. Zuo, G. Li, T. Liu, J. Xiao, Y. Cheng, C. Wang, J.-G. Zhang, J. Liu, *Nano Letters*, **14** (1) , 255 (2014).
9. R. Salomone, F. Mondello, F. Lanuzza, G. Micali, *Environmental Management*, **35** (2) , 206 (2005).
10. K. Periyapperuma, T.T. Tran, S. Trussler, D. Ioboni, M.N. Obrovac, *Journal of the Electrochemical Society*, **161** (14) , A2182 (2014).
11. S.D. Beattie, T. Hatchard, A. Bonakdarpour, K.C. Hewitt, J.R. Dahn, *Journal of the Electrochemical Society*, **150** (6) , A701 (2003).
12. L.D. Ellis, T.D. Hatchard, M.N. Obrovac, *Journal of the Electrochemical Society*, **159** (11) , A1801 (2012).
13. L.D. Ellis, B.N. Wilkes, T.D. Hatchard, M.N. Obrovac, *Journal of the Electrochemical Society*, **161** (3) , A416 (2014).
14. J.-S. Bridel, S. Grugeon, S. Laruelle, J. Hassoun, P. Reale, B. Scrosati, J.-M. Tarascon, *Journal of Power Sources*, **195** (7) , 2036 (2010).
15. B. C. Gerstein, F.J. Jelinek, M. Habenschuss, W.D. Shickell, J.R. Mullaly, P.L. Chung, *The Journal of Chemical Physics*, **47** (6) , 2109 (1967).

1
2
3
4
5
6
7
8
9
10
11
12
13
14
15
16
17
18
19
20
21
22
23
24
25
26
27
28
29
30
31
32
33
34
35
36
37
38
39
40
41
42
43
44
45
46
47
48
49
50
51
52
53
54
55
56
57
58
59
60
61
62
63
64
65

16. A.J. Smith, J.C. Burns, X. Zhao, D. Xiong, J.R. Dahn, *Journal of The Electrochemical Society*, **158** (5) , A447 (2011).
17. Z. Lu, a. Schechter, M. Moshkovich, D. Aurbach, *Journal of Electroanalytical Chemistry*, **466** (2) , 203 (1999).
18. I. Courtney, J. Tse, O. Mao, J. Hafner, J. Dahn, *Physical Review B*, **58** (23) , 15583 (1998).
19. J. Dahn, I. Courtney, O. Mao, *Solid State Ionics*, **111** , 289 (1998).

Figure 1

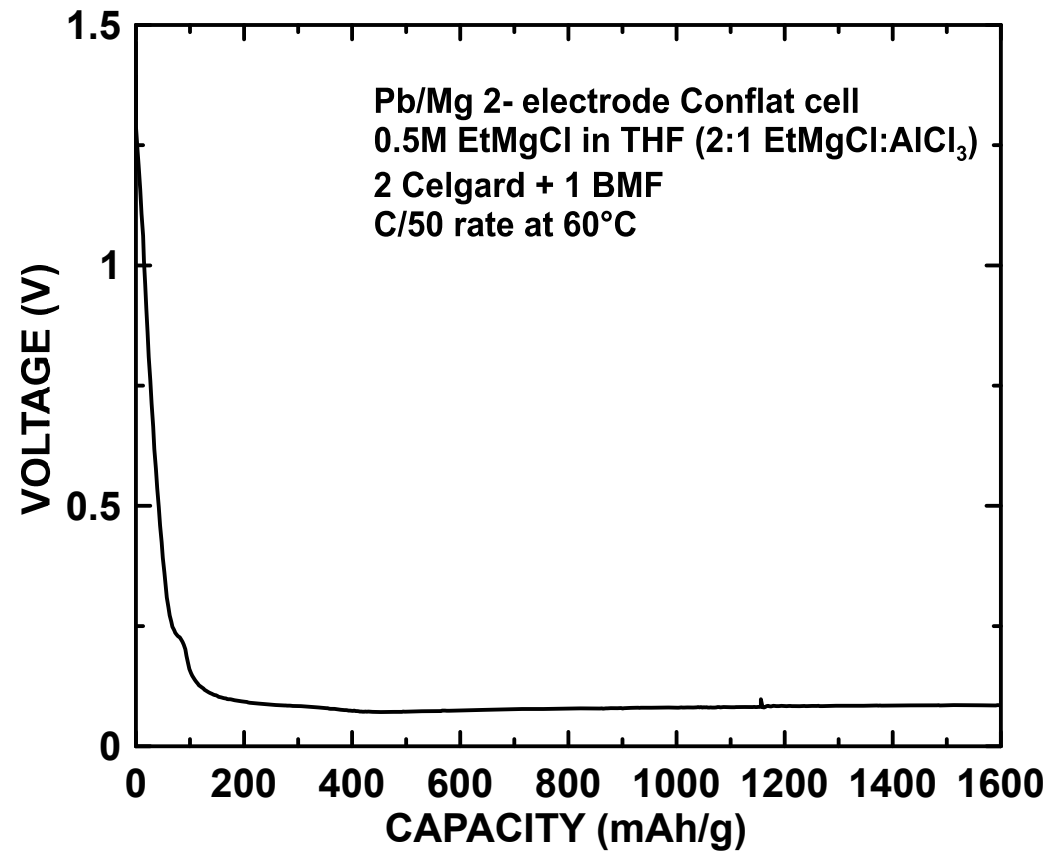


Figure 2

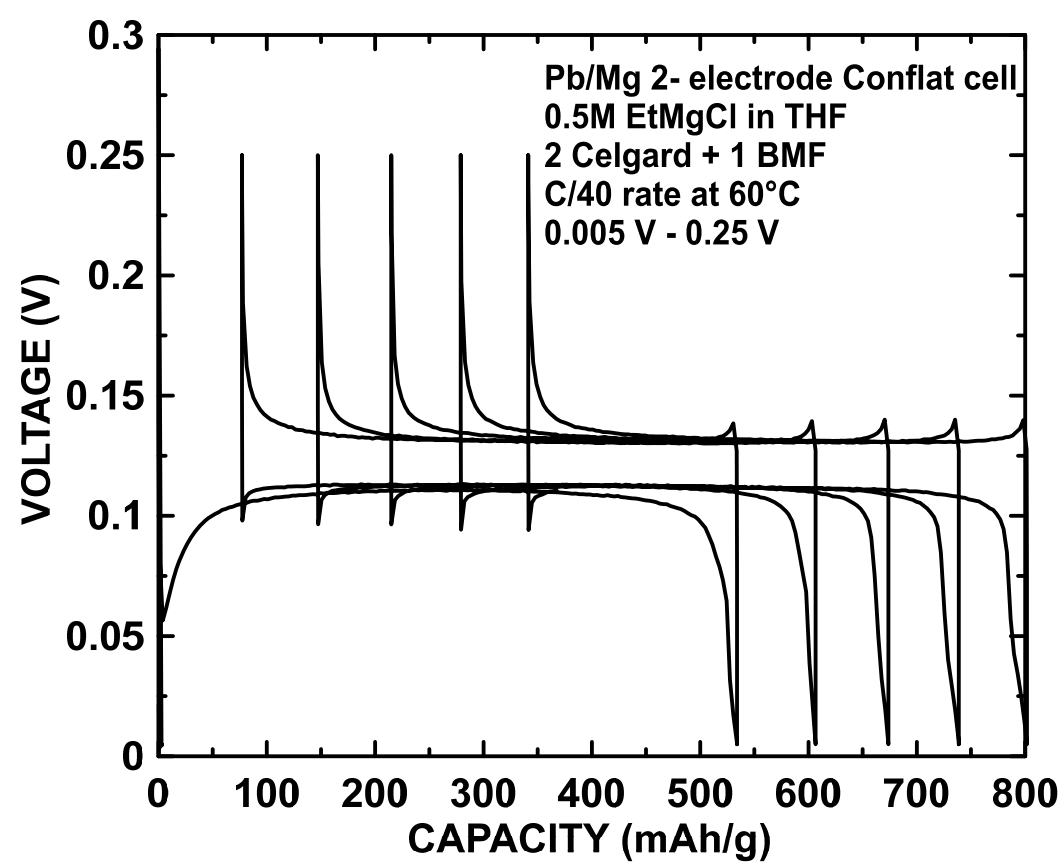


Figure 3

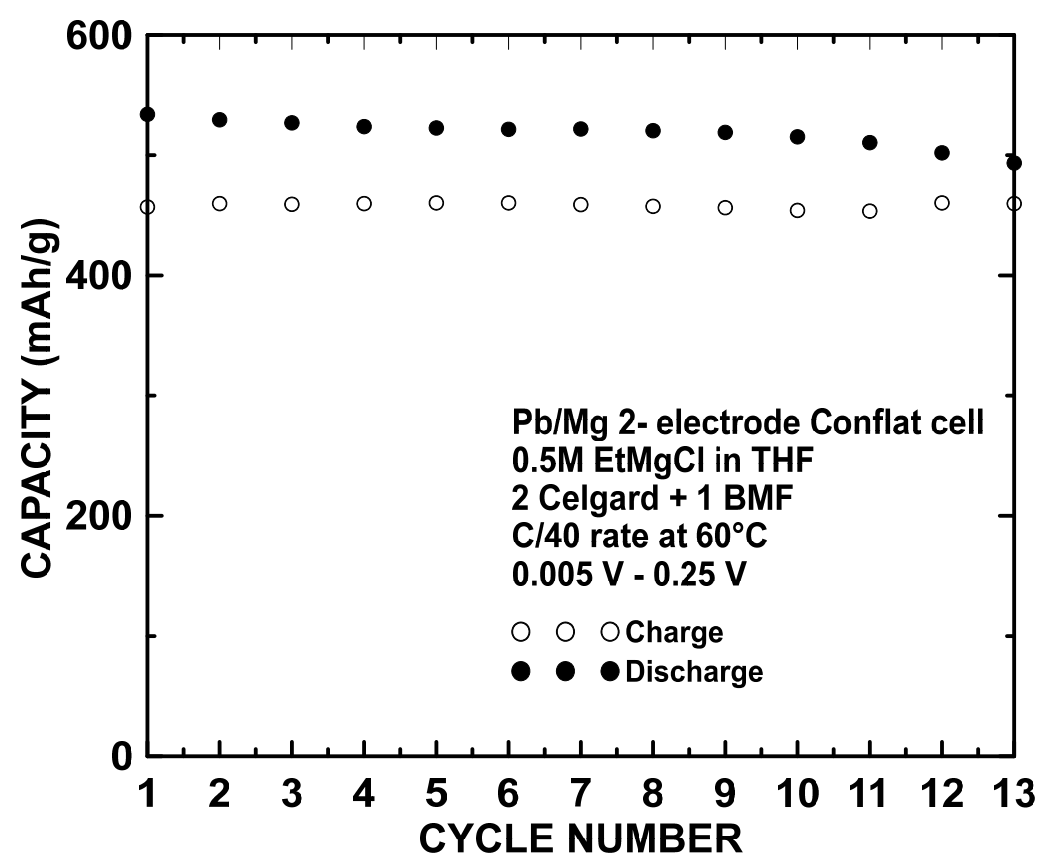


Figure 4

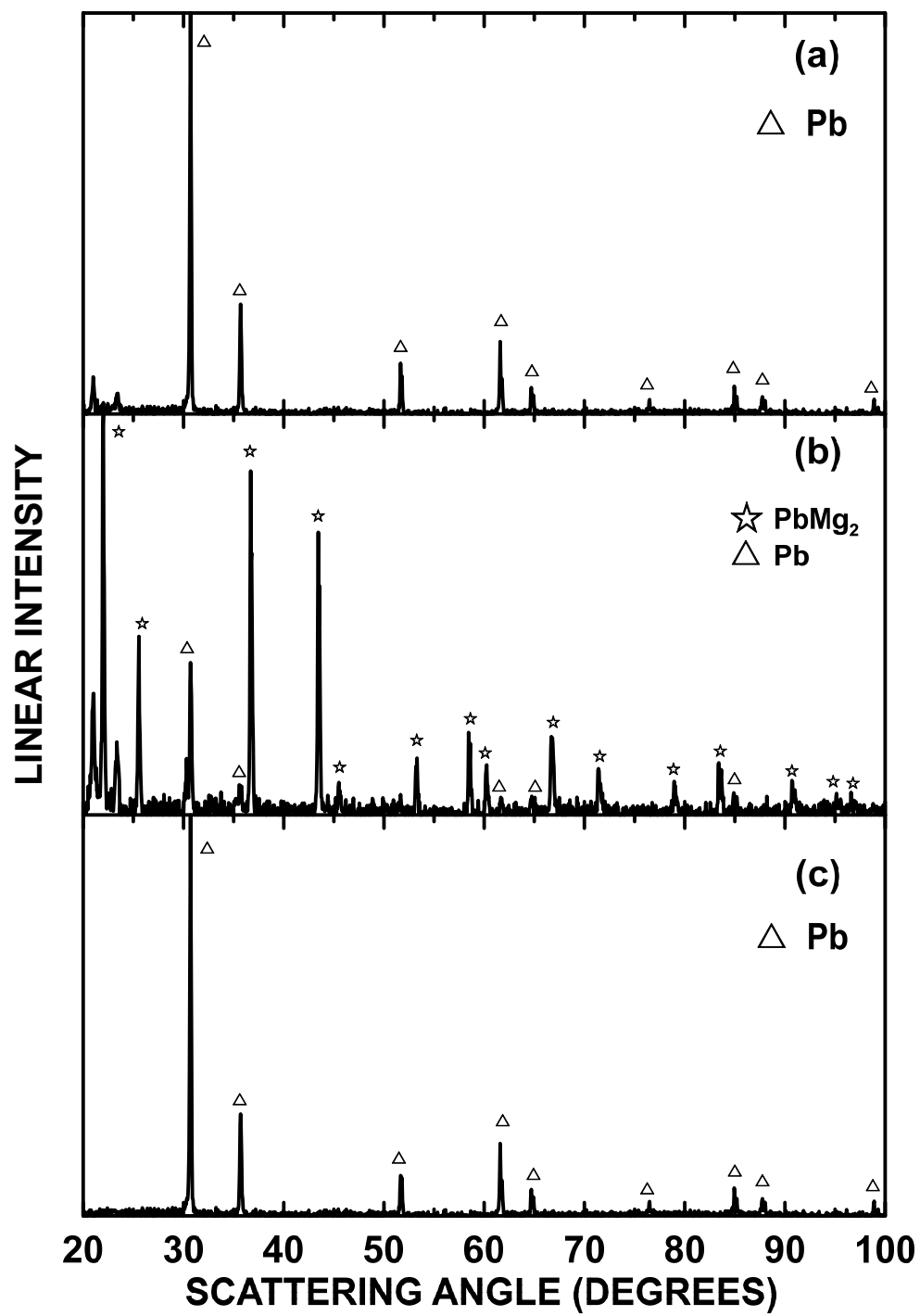


Figure 5

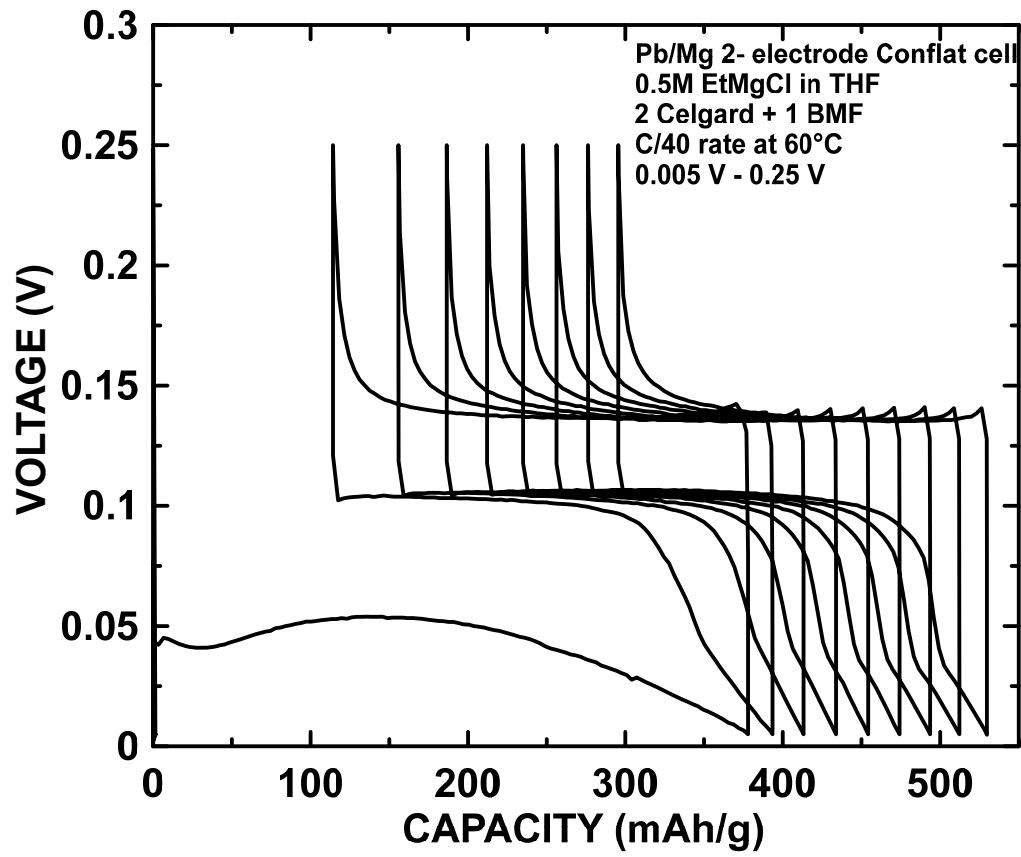


Figure 6

